CrystEngComm

Accepted Manuscript

ROYAL SOCIETY OF CHEMISTRY

www.rsc.org/crystengcomm

Cite this: DOI: 10.1039/c0xx00000x

www.rsc.org/xxxxxx

ARTICLE TYPE

A series of lanthanide−organic frameworks possessing arrays of 2D intersecting channels within a 3D pillar-supported packed double-decker network and Co^{2+}-induced luminescence modulation†

Yen-Hsiang Liu,* and Po-Hsiu Chien

Received (in XXX, XXX) Xth XXXXXXXXX 20XX, Accepted Xth XXXXXXXXX 20XX
DOI: 10.1039/b000000x

A new family of three-dimensional lanthanide metal–organic frameworks (Ln-MOFs) formulated as $\{Ln(NDC)_{1.5}(DMF)(H_2O)_{0.5}\cdot 0.5DMF\}n$ (Ln = Ce, Pr, Nd, Eu; DMF = *N*,*N*′-dimethylformamide; NDC = 2,6-naphthalenedicarboxylic acid) (**FJU6**) was prepared using a combination of extended dicarboxylate ligands and lanthanide cations under mild hydrothermal conditions. **FJU6** contains a rare packed double-decker unit. The adjacent packed double-decker units are further pillared by NDC ligands through different coordination modes, resulting in the generation of a porous 3D framework. Notably, arrays of two-dimensional intersecting channels, occupied by coordinated and guest DMF molecules, are found in **FJU6**. Strong hard acid–hard base interactions between Ln^{3+} cations and NDC^{2-} anions, along with strong π−π interactions, were observed between packed 2D double-decker architectures, resulting in a high thermal stability of **FJU6** as evidenced by TG analysis. The structural diversity and photoluminescence properties of the frameworks were also investigated. Significantly, in the case of **Eu-FJU6**, the apparent luminescence modulation induced by presence of diverse amounts of cobalt cations is observed.

Introduction

Over the past decade, considerable efforts have been made toward the construction and investigation of lanthanide-based metal–organic frameworks (Ln-MOFs), not only because of their exceptional coordination properties and structural diversity but also their intriguing luminescence and magnetism behaviour.[1] Therefore, research into Ln-MOFs with emphasis on certain topics such as optical imaging, solid-state lighting, and sensor materials has been well documented.[2–4] Two well-known features, as compared with transition metal ions, are that lanthanide ions have higher coordination numbers and more versatile coordination geometries, making controlling the self-assembly of Ln-MOFs with desired structural properties and specific porosity a challenge until now. Moreover, lanthanide contraction may exert a noticeable effect on the formation of Ln-MOFs through diverse coordination characristics.[5]

It is generally acknowledged that the so-called "pillaring strategy",[6] which is achieved by the judicious use of a combination of two types of functional ligands, can be regarded as an excellent method for fabricating first-row transitions metal–organic frameworks (TRs-MOFs) featuring highly unique and porous three-dimensional (3D) networks. However, strategies for the design of "pillar-layered" or "layer-pillared" 3D Ln-MOFs are still limited.[7] Although reported, hitherto, Ln-MOFs based on a mixed-type of organic ligand assembly system usually possess a well-defined two-dimensional layer in the host frameworks,[8] examples of Ln-MOFs that exhibit a 2D double-decker motif are quite rare.[9] To the best of our knowledge, 3D Ln-MOFs and/or MOFs that are self-assembled by a pillaring strategy can be classified into three categories (Scheme 1). In type (I) and type (II) networks,[7,10] the components that contribute to the construction of the layer-pillared structure are similar, but a major distinction between them is the presence of non-covalent interactions. In type (III) networks,[9] the 2D monolayer unit is replaced by a 2D double-decker unit, which is normally connected by reacting ligands. In this study, **FJU6** is comprised of a unique 2D packed double-decker unit, a structure that is observed for the first time.

Moreover, it is not uncommon that the construction of Ln-MOFs completed by pillaring a 2D monolayer or a 2D double-decker can generate one-dimensional (1D) porous channels that can accommodate guest molecules, only a few examples of Ln-MOFs containing a two-dimensional intersecting channels system built upon a single type of reacting organic ligand are available.[11] It would be expected that utilizing aromatic ring-based carboxylate ligands and lanthanide cations under appropriate hydrothermal conditions would result in the formation of porous Ln-MOFs with unusual structural peculiarities, because the rigid nature of the ligand conformation and, undoubtedly, hard acid–hard base interactions between carboxylate oxygen atoms and lanthanide cations would further stabilize the host frameworks without the addition of ancillary ligands for enhancing structural diversity. In this context, we report herein on the preparation of a new class of Ln-MOFs, **FJU6**, a 3D layer-

pillared structure composed of a single type of organic ligand (2,6-NDC) and lanthanide cations (Ce, Pr, Nd, and Eu), leading to arrays of two-dimensional intersecting channels embedded in a 3D pillar-supported packed double-decker architecture. Strong π − π interactions are particularly crucial factors in the stability of the host frameworks along with the creation of unique packing units derived from two sets of 2D double-deckers. This fascinating structural feature is observed for the first time and is very different from other lanthanide-based metal–organic frameworks. Aside from documenting the structural distinctiveness of such frameworks, **Eu-FJU6** exhibits luminescence modulation in response to the inclusion of distinct amounts of Co^{2+} ions in aqueous solution under a reflux activation process, as a result of the metal − Lewis basic carboxylate site interactions that functioned in the **Eu-FJU6**⊃Co^{2+} complex.[12]

Scheme 1.

Scheme 1. The general classification of layer-pillared 3D metal–organic frameworks: type (I), MOFs are composed of prerequisite components; type (II), MOFs are composed of the same components as in type (I), but a pillared-bilayer structure can be formed by supramolecular interactions; type(III), MOFs are composed of the same components as in type (I), but a double-decker is substituted for a monolayer. In this study, **Ce-FJU6** is composed of the same components as in type (I), but a structural novelty is additionally introduced in **Ce-FJU6** by a pillar-supported packed double-decker unit and arrays of 2D intersecting channels.

Experimental Section

Material and general methods

All reagents and reactants were purchased commercially and were used directly without any purification. Elemental analyses (C, H, N) were performed on a Perkin-Elmer 2400 elemental analyzer. Fourier transform infrared (FTIR) spectra were recorded on a Perkin-Elmer Spectrum 100 FTIR spectrometer equipped with an attenuated total reflection (ATR) device in the range of 4000 − 650 cm^{-1}. Absorption peaks are reported as follows: very strong (vs), strong (s), medium, (m), weak (w). Thermogravimetric (TG) analyses were performed on a Perkin-Elmer TGA 7 thermogravimetric analyzer with a heating rate of 5 °C/min^{-1} under a nitrogen atmosphere with a flow rate of 20 ml/min. Powder X-Ray Diffraction (PXRD) patterns were recorded on a Philips X'Pert powder X-ray diffractometer at 40 kV, 30 mA with Cu-$K\alpha$ (λ = 1.5406 Å) under step mode with a fixed time of 1s and a step size of 0.02° in 2θ. The photoluminescence (PL) spectra of 2,6-NDC, **Eu-FJU6**, desolvated **Eu-FJU6**, and guest inclusion samples were recorded on a Perkin-Elmer LS55 fluorescence spectrometer at room temperature. The quantum yield measurements were determined at room temperature on a Horiba Jobin Yvon Fluorolog-3 FL3-21 spectrophotometer with an integrating sphere. Lifetime measurements were carried out at room temperature using a FL920 from Edinburgh Instruments.

Synthesis of $Ce(NDC)_{1.5}(DMF)(H_2O)_{0.5}$·0.5DMF (Ce-FJU6)

A solution containing a mixture of $Ce(NO_3)_3·6H_2O$ (56.4 mg, 0.13 mmol), 2,6-naphthalenedicarboxylic acid (H_2NDC, 32.4 mg, 0.15 mmol) and DMF / MeOH / H_2O (4 / 2 / 1 ml) was sealed in a 23 mL Teflon-lined vessel which was then heated at 95 °C for 12 hours under hydrothermal conditions. The yellowish, needle-liked crystals of **Ce-FJU6** that were obtained were washed with DMF (5 ml). The solid crystals of **Ce-FJU6** were found to be suitable for single-crystal X-ray analyses and phase purity was further verified by comparison with a simulated Powder X-Ray Diffraction pattern from single-crystal X-ray diffraction data of **Ce-FJU6**. Yield: 40.2 %, based on the Ce salt content. Elemental analysis Calcd. for $C_{22.5}H_{20.5}N_{1.5}O_8Ce$: C, 46.59; H, 3.56; N, 3.62. Found: C, 46.48; H, 3.44; N, 3.23. IR (ATR-IR): ν = 1667 (m), 1609 (m), 1557 (s), 1490 (m), 1397 (vs), 1360 (vs), 1251 (w), 1201 (m), 1188 (m), 1140 (w), 1104 (m), 1062 (w), 974 (w), 969 (w), 922 (m), 867 (w), 849 (w), 832 (w), 799 (w), 789 (s), 775 (s), 752 (w), 671 (m) cm^{-1}.

Synthesis of $Pr(NDC)_{1.5}(DMF)(H_2O)_{0.5}$·0.5DMF (Pr-FJU6)

A solution containing a mixture of $Pr(NO_3)_3·6H_2O$ (56.4 mg, 0.13 mmol), 2,6-naphthalenedicarboxylic acid (H_2NDC, 32.3 mg, 0.15 mmol) and DMF / MeOH / H_2O (4 / 2 / 1 ml) was sealed in a 23 mL Teflon-lined vessel and was then heated at 95 °C for 12 hours under hydrothermal conditions. The pale green, needle-liked crystals of **Pr-FJU6** that were obtained were washed with DMF (5 ml). The microcrystalline powder of **Pr-FJU6** was further verified by comparison with a simulated Powder X-Ray Diffraction pattern from single-crystal X-ray diffraction data of **Ce-FJU6**. Yield: 38.2 %, based on the Pr salt content. Elemental analysis Calcd. for $C_{22.5}H_{20.5}N_{1.5}O_8Pr$: C, 46.52; H, 3.55; N, 3.61. Found: C, 46.12; H, 3.46; N, 3.80. IR (ATR-IR): ν = 1668 (m), 1610 (m), 1558 (s), 1491 (m), 1399 (vs), 1361 (vs), 1253 (w), 1201 (m), 1188 (m), 1141 (w), 1105 (m), 1062 (w), 957 (w), 969 (w), 922 (m), 869 (w), 848 (w), 832 (w), 800 (w), 790 (s), 775 (s), 752 (w), 672 (m) cm^{-1}.

Synthesis of $Nd(NDC)_{1.5}(DMF)(H_2O)_{0.5}$·0.5DMF (Nd-FJU6)

A solution containing a mixture of $Nd(NO_3)_3·6H_2O$ (57.1 mg, 0.13 mmol), 2,6-naphthalenedicarboxylic acid (H_2NDC, 32.6 mg, 0.15 mmol) and DMF / MeOH / H_2O (4 / 2 / 1 ml) was sealed in a 23 mL Teflon-lined vessel and was then heated at 95 °C for 12 hours under hydrothermal conditions. The pale violet, needle-liked crystals of **Nd-FJU6** that were obtained were washed with DMF (5 ml). The microcrystalline powder of **Nd-FJU6** was further verified by comparison with a simulated Powder X-Ray Diffraction pattern from single-crystal X-ray diffraction data of **Ce-FJU6**. Yield: 38.3 %, based on the Nd salt content. Elemental analysis Calcd. for $C_{22.5}H_{20.5}N_{1.5}O_8Nd$: C, 46.26; H, 3.53; N, 3.59. Found: C, 45.57; H, 3.44; N, 3.79. IR (ATR-IR): ν = 1668 (m), 1610 (m), 1558 (s), 1491 (m), 1400 (vs), 1361 (vs), 1253 (w), 1201 (m), 1188 (m), 1141 (w), 1105 (m), 1062 (w), 975 (w), 969 (w), 922 (m), 868 (w), 848 (w), 831 (w), 801 (w), 789 (s), 775 (s), 751 (w), 672 (m) cm^{-1}.

Synthesis of $Eu(NDC)_{1.5}(DMF)(H_2O)_{0.5}$·0.5DMF (Eu-FJU6)

A solution containing a mixture of $Eu(NO_3)_3·6H_2O$ (44.8 mg, 0.1 mmol), 2,6-naphthalenedicarboxylic acid (H_2NDC, 32.5 mg, 0.15 mmol) and DMF / MeOH / H_2O (4 / 2 / 1 ml) was sealed in a 23 mL Teflon-lined vessel and was then heated at 95 °C for 12 hours under hydrothermal conditions. The resulting yellowish, tiny grain crystalline powder of **Eu-FJU6** that was obtained was washed with DMF (5 ml). The microcrystalline powder of **Eu-FJU6** was further verified by comparison with a simulated

Powder X-Ray Diffraction pattern from single-crystal X-ray diffraction data of **Ce-FJU6**. Yield: 47.1 %, based on the Eu salt content. Elemental analysis Calcd. for $C_{22.5}H_{20.5}N_{1.5}O_8Eu$: C, 45.65; H, 3.49; N, 3.54. Found: C, 45.71; H, 3.25; N, 3.80. IR (ATR-IR): ν = 1656 (m), 1607 (m), 1555 (s), 1492 (m), 1404 (vs), 1358 (s), 1255 (w), 1203 (m), 1192 (m), 1141 (w), 1109 (m), 1089 (m), 1063 (w), 932 (m), 920 (m), 866 (w), 835 (w), 806 (m), 791 (s), 774 (s), 750 (w), 677 (m) cm^{-1}.

Preparation of desolvated Eu-FJU6

A 50 mg sample of a well-ground powder of **Eu-FJU6** in 30 ml of deionized water was heated in a reflux apparatus at 90 °C for 24 hours. After cooling to room temperature, the bulk samples were collected on a filter, washed with deionized water (100 ml), and dried under aerobic conditions for 3 days. The desolvated sample was further examined by Powder X-Ray Diffraction (PXRD) analysis (Fig. S1),† and Fourier transform infrared (FTIR) spectra (Fig. S2)† to verify its phase purity as well as the absorption peaks of the coordinated *N*,*N*′-dimethylformamide (DMF) molecules.

Preparation of guest-inclusion sample of Eu-FJU6⊃cation

A mixture of 80 mg of well-ground powder of **Eu-FJU6**, and 30 ml of an aqueous metal ion solution of $M(NO_3)_x$ (x = 1 or 2, M = Na^+, Co^{2+}, Ni^{2+}, Cu^{2+}, Zn^{2+}, Cd^{2+}) prepared by dissolving metal nitrate in deionized water at sequentially diluted concentrations, was heated at 90 °C in a reflux apparatus for 24 hours. After cooling to room temperature, the bulk samples were collected on a filter, washed with deionized water (100 ml), and dried under aerobic conditions for 3 days.

Crystallographic measurements

A single crystal of **Ce-FJU6** suitable for X-ray diffraction was placed in a cooled N_2 gas stream at ~200 K for intensity data collection on a Bruker APEX-II CCD diffractometer with graphite monochromated Mo-Kα (λ = 0.71073 Å) radiation. Data reduction included absorption corrections by the MULTISCAN method, using the Bruker SAINT[13] and SADABS.[14] Crystal data and experimental details are given in Table 1. The X-ray structure was determined by direct methods and difference Fourier techniques and refined by full-matrix least squares, using the SHELXL97 program.[15] All non-hydrogen atoms were refined anisotropically except for the O22 atom of the carboxylate group of one of the NDC ligand. Attempts to perform an anisotropic refinement of the O(22) atom were unsuccessful, which can be attributed to the large residue density around the Ce centre, it was only possible to perform an isotropic refinement for the O(22) atom.

The atoms of the terminally coordinated DMF molecule showed large anisotropic displacement parameters due to the disordered nature of the guest molecules that could move or vibrate around the O(41)---Ce(1) coordination bond. The free DMF molecule resided on the crystallographic twofold rotation symmetry through the C(51) and N(51) atoms of the free DMF molecule, and present a two-site disorder nature. As a result, O(51) atom of the aldehyde group of the free DMF molecule is two-site disordered with site-occupancy-factor (S. O. F.) to be 0.5. Also, the assignment of the H atom position of the aldehyde group of the DMF molecule is not attempted due to the two-site disorderness with the O(51) atom of the aldehyde group of DMF molecule. Also, the atoms of the free DMF molecule show large anisotropic displacement parameters because of the disorderness. The C-bound, and O-bound H atoms were placed in the calculated positions and refined by a riding-model approximation. Crystallographic data structures for **Ce-FJU6** have been deposited at the Cambridge Crystallographic Data Centre, under the deposition number CCDC 989479.

Table 1. Crystallographic data and structure refinement summary for **Ce-FJU6**

Chemical formula	$Ce(NDC)_{1.5}(DMF)(H_2O)_{0.5}\cdot 0.5DMF$
a, Å	12.4814(1)
b, Å	21.763(3)
c, Å	16.509(2)
α, deg	90
β, deg	103.577(5)
γ, deg	90
U, $Å^3$	4539(1)
Z	4
M	580.0
Space group	*C*2/*c*
T, K	293(2)
λ, Å	0.71073
D_{calcd}, g/cm^3	1.768
Refls measured	13862
Independent Refls	3932 [$R(int)$ = 0.1254]
μ, cm^{-1}	2.14
$R1^a$ [$I > 2\sigma(I)$]	0.0728
$wR2^a$ (all data)	0.1597

$^a R1 = \sum||F_o|-|F_c||/\sum|F_o|$ $wR2 = \{\sum[w(F_o^2-F_c^2)^2]/\sum[w(F_o^2)^2]\}^{1/2}$

Results and Discussion

Preparation

It seems to be generally accepted that hydro(solvo)thermal conditions play a vital role in the construction of kaleidoscopic crystal structures because of the higher reaction temperature and pressure that can be achieved in a sealed Teflon-lined stainless steel vessel, under hydro(solvo)thermal conditions. This makes it possible to advance crystal engineering more rapidly as a result of the elevated solubility of the resulting materials, which improves reactivity as a whole and has stimulated researchers to experiment with a wider range of combination of factors.[16] Under mild hydrothermal conditions, it was possible to produce $[Ln(NDC)_{1.5}(DMF)(H_2O)_{0.5}\cdot 0.5DMF]_n$ **(FJU6)**. The formula of **FJU6** was confirmed by single-crystal X-ray diffraction, elemental and thermogravimetric analyses. The temperature factor and solvent ratio between DMF, methanol, and water plays an important role in controlling the phase purity and yield of the bulk product. At a higher reaction temperature of about 150 °C, the phase purity and yield of **FJU6** are retained even in the absence of the methanol solvent. The addition of methanol to the reaction has a stimulatory effect on the growth of good quality crystal products for single crystal X-ray diffraction analysis, and to help in maintaining the phase purity and yield of **FJU6** when the reaction temperature is lowered to about 95 °C.

A tender method called reflux activation, which functions at temperatures below 100 °C, was developed to hydrolyze stubbornly coordinated or guest DMF molecules for producing active sites and for conducting experiments related to metal-

induced luminescence modulation in aqueous solution. Also, reflux activation was used to prepare desolvated **Eu-FJU6** and a guest-inclusion sample of **Eu-FJU6**⊃cation.

Structural Description

The results of powder X-ray diffraction analyses (Fig. S3)† show that all of the four lanthanide–organic frameworks are isomorphous, and thus only the structural details of **Ce-FJU6** are described here. A single crystal X-ray diffraction analysis revealed that **Ce-FJU6** crystallizes in a space group *C*2/*c* of monoclinic unit cell. The crystallographic asymmetric unit of **Ce-FJU6** contains one unique Ce^{3+} ion, one coordinated DMF molecule, three half NDC^{2-} ligands, one lying about an inversion center while the other two lie about independent two-fold axes, a bridging water molecule (O99) lying on a two-fold axis, and the non-coordinated DMF of solvation also lies about a two-fold axis. Therefore, the formula of **Ce-FJU6** is $[Ce(NDC)_{1.5}(DMF)(H_2O)_{0.5}\cdot 0.5DMF]_n$ (Fig. S4).† For the NDC^{2-} ligands, all of the carboxylate groups are completely deprotonated, thus neutralizing the positive charges of the Ce^{3+} ions, which is in good agreement with IR spectral data (Fig. S5)† which show no strong absorption peaks corresponding to the carbonyl group in **FJU6** at around 1715–1680 cm^{-1}.[17]

As shown in Fig. 1, each type of bridging NDC^{2-} ligand binds to four Ce^{3+} ions with two distinct types of coordination modes, namely, type-I, a bis(syn,syn-bridging bidentate) coordination mode (NDC^{I}-a and NDC^{I}-b), and a bis(chelating-bridging bidentate) coordination mode (NDC^{II}). A center of symmetry is observed for each type of NDC^{2-} ligand. It is noteworthy that different degrees of distortion of the carboxylate groups with respect to the naphthalene rings of NDC^{I} and NDC^{II} ligands are observed.

Fig. 1.

Fig. **1**. The coordination modes of NDC^{2-} ligand: type-I, bis(syn,syn-bridging bidentate) (top and middle); type-II, bis(chelating-bridging bidentate) (bottom); torsion angle: $\alpha = 7.24°$; $\alpha' = 11.96°$; $\beta = 17.71°$; $\beta' = 20.80°$; $\gamma = 7.75°$; $\gamma' = 5.69°$. Key: green, Ce; pink, C in NDC^{I}; darkblue, C in NDC^{II}; red, O; all the H atoms are omitted for clarity. Symmetry transformations used to generate equivalent atoms: (iii) *1 – x*, *y*, *– 0.5 – z*; (iv) *1.5 – x*, *0.5 – y*, *– z*; (v) *1 – x*, *y*, *0.5 – z*.

In the case of **Ce-FJU6**, the coordination sphere of the cerium cation adopts a distorted monocapped square antiprism, consisting of a nine-coordinated Ce^{3+} centre (Fig. 2a). The Ce^{3+} centre is surrounded by nine oxygen atoms, which are attributed to one bridged water molecule (O99), one coordinated DMF molecule (O41), four monodentate carboxylate groups of NDC^{I} ligands (O11, O12i, O31, O32ii), and one chelating carboxylate group of NDC^{II} ligand (O21) and O(22) and one monodentate carboxylate group of NDC^{II} ligand (O22i) (Fig. 2b). The Ce–O bond lengths and O–Ce–O bond angles for Ce^{3+} coordination spheres are within the ranges of 2.377(7)–2.808(7) Å and 47.6(2)–148.5(3)°, respectively, as shown in Table 2. Importantly, two nine-coordinated Ce^{3+} ions form an edge-sharing Ce_2O_9 polyhedron moiety through O22–O22(i) bonding, and this moiety can be envisaged as a secondary building unit (Ce_2-unit) in which a centre of symmetry can be observed.

Fig. 2.

Fig. **2**. (a) The distorted monocapped square antiprismatic coordination sphere of the Ce^{3+} ion. (b) A polyhedral view of Ce_2O_9 polyhedron (Ce_2-unit). Key: green, Ce; pink, C in NDC^{I}; darkblue, C in NDC^{II}; red, O; aqua, water molecule; all the H atoms are omitted for clarity. Symmetry transformations used to generate equivalent atoms: (i) *2 – x*, *– y*, *– z*; (ii) *2 – x*, *y*, *0.5 – z*.

Each Ce_2-unit is further bridged by one water molecule (O99) as well as two syn-bridging carboxylate groups (O31 and O32) of NDC^{I}-a ligands to form a one-dimensional Ce–carboxylate cluster chain along the crystallographic *c*-direction, as illustrated in Fig. 3. The Ce^{3+} ions are arranged in a Ce···Ce*···Ce sequence with alternating intermetallic distances of 4.092 and 4.841 Å. The delicate assembly of the 1D Ce–carboxylate cluster chains can be attributed to the embedding of bridged water molecules and its temperate hydrogen-bonding interactions with bridging carboxylate groups. The hydrogen-bonding interactions between bridged water molecules (O99) to the oxygen atoms (O12 in NDC^{I}-b and O21 in NDC^{II}) of the carboxylate groups are observed, as shown in Fig. S6† and Table 3.

Table 2. Selected bond lengths [Å] and angles [°] for Ce^{3+} coordination environments in **Ce-FJU6**

Ce(1)–O(31)	2.376(7)	O(12)$^{\#1}$–Ce(1)–O(41)	137.1(3)
Ce(1)–O(11)	2.421(7)	O(31)–Ce(1)–O(21)	76.6(3)
Ce(1)–O(22)$^{\#1}$	2.456(7)	O(11)–Ce(1)–O(21)	76.2(3)
Ce(1)–O(32)$^{\#2}$	2.462(7)	O(22)$^{\#1}$–Ce(1)–O(21)	125.5(2)
Ce(1)–O(12)$^{\#1}$	2.479(7)	O(32)$^{\#2}$–Ce(1)–O(21)	139.6(3)
Ce(1)–O(41)	2.583(8)	O(12)$^{\#1}$–Ce(1)–O(21)	88.6(3)
Ce(1)–O(21)	2.585(7)	O(41)–Ce(1)–O(21)	134.2(2)
Ce(1)–O(99)	2.669(5)	O(31)–Ce(1)–O(99)	68.4(2)
Ce(1)–O(22)	2.808(7)	O(11)–Ce(1)–O(99)	136.8(2)
O(31)–Ce(1)–O(11)	86.2(3)	O(22)$^{\#1}$–Ce(1)–O(99)	138.5(2)
O(31)–Ce(1)–O(22)$^{\#1}$	148.4(3)	O(32)$^{\#2}$–Ce(1)–O(99)	75.1(2)
O(11)–Ce(1)–O(22)$^{\#1}$	79.1(2)	O(12)$^{\#1}$–Ce(1)–O(99)	65.1(2)
O(31)–Ce(1)–O(32)$^{\#2}$	89.2(2)	O(41)–Ce(1)–O(99)	126.1(3)
O(11)–Ce(1)–O(32)$^{\#2}$	141.2(3)	O(21)–Ce(1)–O(99)	64.6(2)
O(22)$^{\#1}$–Ce(1)–O(32)$^{\#2}$	85.1(2)	O(31)–Ce(1)–O(22)	121.5(2)
O(31)–Ce(1)–O(12)$^{\#1}$	133.2(3)	O(11)–Ce(1)–O(22)	67.3(2)
O(11)–Ce(1)–O(12)$^{\#1}$	133.4(3)	O(22)$^{\#1}$–Ce(1)–O(22)	78.2(2)
O(22)$^{\#1}$–Ce(1)–O(12)$^{\#1}$	74.6(3)	O(32)$^{\#2}$–Ce(1)–O(22)	143.0(2)
O(32)$^{\#2}$–Ce(1)–O(12)$^{\#1}$	73.8(3)	O(12)$^{\#1}$–Ce(1)–O(22)	70.0(2)
O(31)–Ce(1)–O(41)	70.3(3)	O(41)–Ce(1)–O(22)	135.1(3)
O(11)–Ce(1)–O(41)	71.0(3)	O(21)–Ce(1)–O(22)	47.6(2)
O(22)$^{\#1}$–Ce(1)–O(41)	78.4(3)	O(99)–Ce(1)–O(22)	96.2(3)
O(32)$^{\#2}$–Ce(1)–O(41)	71.2(3)		

Symmetry transformations used to generate equivalent atoms: (#1) *2 – x*, *– y*, *– z*; (#2) *2 – x*, *y*, *0.5 – z*.

Table 3. Selected Hydrogen Bonding Interactions in **Ce-FJU6**

donor–H···acceptor	D–H (Å)	H···A (Å)	D···A (Å)	donor–H···A (deg)
O(99)–H(99A)···O(21)	0.85	2.18	2.808(8)	130
O(99)–H(99A)···O(51ii)	0.85	2.08	2.61(4)	120

Symmetry transformations used to generate equivalent atoms: (ii) *2 – x*, *y*, *0.5 – z*.

Significantly, the disparate coordination modes of the NDC^{2-} ligands not only aid in the construction of the Ce_2-unit and 1D Ce–carboxylate cluster chains but also serve as double spacers with NDC^{I} ligands to further interconnect the neighboring 1D Ce–carboxylate cluster chains into a two-dimensional packed double-decker that expands along the crystallographic *ac*-plane (Fig. 3 and Fig. S7).† Differing from the layer-pillared Ln-MOFs constructed by 2D double-deckers in the literature,[9] the packed 2D double-deckers found in **Ce-FJU6** are built by arranging two

sets of double-decker in a sandwich way as illustrated by Fig. S7.† Each set of single double-decker (skyblue) is intercalated in the centre of another single double-decker (orange), and this packing diagram of double-deckers is observed for the first time for Ln-MOFs. In comparison to the reported layer-pillared Ln-MOFs possessing 2D double-deckers,[9] the formation of each single double-decker is achieved only by the bonding between Ce^{3+} ions and carboxylate groups of NDC^{I} ligands. This is quite dissimilar to previous results for Ln-MOFs contain 2D double-deckers, which were built by bridging or connecting monolayers with ancillary ligands. Interestingly, the strong $\pi-\pi$ interactions of NDC^{I} ligands between the nearly parallel naphthalene rings (C32−C33−C34−C35−C36−C32′−C33′−C34′−C35′−C36′ and C12−C13−C14−C15−C16−C12′−C13′−C14′−C15′−C16′) that were measured showing a centroid…centroid distance of 3.403 Å along the crystallographic *b*-direction. The extension of $\pi-\pi$ interactions along with the formation of 1D Ce–carboxylate cluster chains effectively increase the robustness of the packed 2D double-deckers as a whole. If the coordinated and guest DMF molecules were ruled out by not considered as part of the framework atoms of **Ce-FJU6**, the PLATON[18] calculations of solvent-accessible volume indicate that 32.7 % of the unit cell volume of the framework of **Ce-FJU6** is able to accommodate the coordinated DMF as well as guest DMF molecules. As shown in Fig. 3, the packed 2D double-deckers are further linked by the slanted pillars through NDC^{II} ligands to generate a three-dimensional layer-pillared framework of **Ce-FJU6** (Fig. S8). The apparent template effect of DMF molecules appears to prevent the host frameworks of **Ce-FJU6** from interpenetration. Concerning the features of large porous channels in **Ce-FJU6**, it should be noted that large porous channels can be observed along the crystallographic [101] and [$\bar{1}$01] directions and are identified as empty void spaces for the inclusion of guest and coordinated DMF molecules (Fig. 4).

Fig. 3.

Fig. 3. Ball-and-stick and rod-packing representations of the 1D Ce-carboxylate cluster chain viewed along the *a*-direction (up); A perspective view of the 2D packed "double-decker" viewed along the *b*-direction. The strong $\pi-\pi$ interactions of adjacent NDC^{I} ligands are highlighted in dark plates, and yellow fragmented lines (middle); A perspective view of the layer-pillared 3D frameworks of **Ce-FJU6** viewed along the c-direction illustrates the triangular 1D porous channels (bottom). Key: green, Ce; pink, C in NDC^{I}; darkblue, C in NDC^{II}; red, O; aqua, water molecule; all the H atoms are omitted for clarity.

Fig. 4.

Fig. 4. Perspective views along the four different directions demonstrate the specific features of the 1D porous channels in **Ce-FJU6**. Key: green, Ce; pink, C in NDC^{I}; darkblue, C in NDC^{II}; red, O; aqua, water molecule; all the H atoms are omitted for clarity.

The intersecting 1D porous channels lead to the formation of two-dimensional porous arrays between the packed 2D double-deckers. (Fig. 5). The existence of 2D porous arrays in **Ce-FJU6** is rare for lanthanide–organic frameworks,[13] particularly for those that are constructed solely using a single type of linear carboxylate-based ligand. Thus, the structure of **Ce-FJU6** is unique. For **Ce-FJU6**, the backbone of the packed 2D double-deckers involves the compact stacking of double spacer (NDC^{I} ligands) *via* $\pi-\pi$ interactions on the right and left side of the 1D Ce–carboxylate cluster chains. More importantly, the configuration of the slanted pillars (NDC^{II} ligands), which are stretched out with a tilted configuration at the top and bottom of the 1D Ce–carboxylate cluster chains, cooperate with the guest and the coordinated DMF molecules to generate the specific features of the porous channels and to stabilize the overall structure. It is probable that the 2D porous arrays of intersecting channels are caused by this sort of dislocation of NDC^{2-} ligands in **Ce-FJU6**. Two La-NDC compounds ($La_2(NDC)_3$(e-urea)$_3$, e-urea = ethyleneurea; $La_2(NDC)_3(DMF)_2\cdot(H_2O)$) possessing distinct types of bridging ligands as well as different coordinated and free guest molecules that are structurally analogous to **Ce-FJU6** ($Ce(NDC)_{1.5}(DMF)(H_2O)_{0.5}\cdot 0.5DMF$) have been reported.[19]

Fig. 5.

Fig. 5. An illustration of the two-dimensional porous array of intersecting channels between the adjacent packed 2D double-deckers of **Ce-FJU6**. Channels openings are observed along the crystallographic [101] and [-101] directions (left and right pictures presented in Connolly surfaces). For clarity, the host frameworks are all depicted in white, and the 2D porous arrays are depicted in yellow (middle). All the H atoms, DMF molecules, and guest molecules are omitted for clarity.

Thermal stability analysis

TG (Thermogravimetric) curves for **Ln-FJU6** (Ln = Ce, Pr, Nd, and Eu) were measured in the temperature range of 25–950 °C under a flow of N_2. As shown in Fig. S9,† **Ln-FJU6** showed a continuous weight loss of 20.0% for **Ce**, 19.8% for **Pr**, 20.3% for **Nd** and 19.3% for **Eu** (calcd: 20.3% for **Ce**, 20.3% for **Pr**, 20.1% for **Nd**, 19.9 % for **Eu**) starting at 30 °C and ending at 420 °C for **Ce**, 470 °C for **Pr**, 440 °C for **Nd**, 440 °C for **Eu**, respectively, which correspond to the loss of one coordinated DMF molecule, 0.5 bridged water molecule, and 0.5 guest DMF molecule per formula weight. It is not uncommon for lanthanide–organic frameworks to demonstrate a high degree of thermal stability, which can be attributed to the rigid bonding between lanthanide ions and oxygen atoms with hard acid−hard basic interactions.[20] In addition, the $\pi-\pi$ interactions between the closely stacked naphthalene rings of the NDC^{I} ligands also play a significant role in stabilizing the entire host frameworks to minimize the thermal vibration of the framework caused by the release of bridged water molecules of the 1D Ce–carboxylate cluster chains.[21]

Photoluminescence studies of Eu-FJU6

Solid-state photoluminescence (PL) spectra of the 2,6-NDC ligand and **Eu-FJU6** were recorded under ambient conditions. A broad band in the region of 400-600 nm (λ_{max} = 452 nm) in the emission spectrum (Fig. S10)† is primarily assigned to the intraligand (IL) $\pi^*-\pi$ transition of 2,6-NDC[17,22] by excitation at 370 nm. On the other hand, the excitation spectrum of **Eu-FJU6**, which displayed a maximum excitation band at 368 nm with the emission fixed at 612 nm, was in good agreement with that for the 2,6-NDC ligand. A series of sharp lines at 578.5, 592.5, 612.5, 650.5, and 698 nm that were assigned to $^5D_0\rightarrow{}^7F_0$, $^5D_0\rightarrow{}^7F_1$, $^5D_0\rightarrow{}^7F_2$, $^5D_0\rightarrow{}^7F_3$, and $^5D_0\rightarrow{}^7F_4$ transitions, respectively, were observed in the emission spectrum of **Eu-FJU6** (Fig. 6). An apparent difference in the intensity between $^5D_0\rightarrow{}^7F_1$ (magnetic dipole, MD) and $^5D_0\rightarrow{}^7F_2$ (electric dipole, ED) transitions, in which the latter was approximately 5 times

stronger than the former, indicates that the Eu^{3+} ions locate in noncentrosymmetric sites.[22a,23] The quantum yields of **Eu-FJU6** in solid state upon excitation at 368 nm is 10.9%; the luminescent lifetime of **Eu-FJU6** was also measured and found to be 1.14 ns. Furthermore, the exactly identical emission spectrum of **Eu-FJU6** collected by excitation at 370 nm compared with that for **Eu-FJU6** when excited at 368 nm indicated that the antenna effect was carried out successfully without being quenched by oscillators such as bridged water molecules.[24] The ligand-based emission at 452 nm disappeared upon excitation at 368 and 370 nm, suggesting that the 2,6-NDC ligand has the ability to sensitize Eu^{3+} ions during the ligand-to-metal energy transfer process.[17a,22a]

Guest-induced photoluminescence modulation of Eu-FJU6

The excitation and photoluminescence (PL) spectra measured at room temperature for the desolvated form of **Eu-FJU6** are

Fig. 6.

Fig. 6. Photoluminescence spectra of **Eu-FJU6** (λ_{ex} = 368 nm).

shown in Fig. S11.† Upon excitation at 368 nm, the desolvated **Eu-FJU6** exhibited the characteristic emissions of the Eu^{3+} ion, originating from the first excited state ($^5D_0$) to the ground multiplet (^7F_J, J = 0–4) at 578.5, 591.5, 615, 651 and 697 nm.[24] A small hump at 425–550 nm was presumably caused by the ligand centered emission band of 2,6-NDC due to weaker bonding between the Eu^{3+} ions and carboxylate groups caused by the distortion of the coordination environment of the Eu^{3+} ions that occurs upon desolvation. Although the desolvated **Eu-FJU6** emitted a relatively weak red light because of the structural distortions caused by desolvation, the characteristic emission band features of the Eu-emission such as sharp line peaks, corresponding peak positions, and the intensity ratio between each peak suggest that the desolvated **Eu-FJU6** still exhibited a strong antenna effect. It therefore appears that desolvated **Eu-FJU6** could serve as a potential candidate for use in sensing experiments.

As illustrated by Fig. 7, it is noteworthy that the luminescence behavior of the guest-inclusion **Eu-FJU6** (**Eu-FJU6**⊃cation) is greatly dependent on the nature of the cation. For **Eu-FJU6**⊃Cu^{2+}, **Eu-FJU6**⊃Zn^{2+}, and **Eu-FJU6**⊃Cd^{2+}, the luminescence intensity was completely quenched. On the other hand, Na^+ ions exerted only a minor influence on the luminescence intensity. It is noteworthy that **Eu-FJU6**⊃Ni^{2+} and **Eu-FJU6**⊃Co^{2+} have a profound effect on cation-dependent luminescence quenching behavior.

Intrigued by the interesting features of the sensing phenomenon as reported in the literature,[25] further studies of the luminescence behavior of **Eu-FJU6**⊃Ni^{2+} and **Eu-FJU6**⊃Co^{2+} in sequentially diluted concentrations of cation solution were performed. As shown in Fig. 8, **Eu-FJU6**⊃Ni^{2+} and **Eu-FJU6**⊃Co^{2+} showed the most significant quenching effect as gradually attenuated by the concentration of Co^{2+} and Ni^{2+} ions, respectively, For **Eu-FJU6**⊃Ni^{2+}, the $^5D_0 \rightarrow {}^7F_2$ luminescence intensity (615 nm) for a 0.5 mol L^{-1} solution was about 5.5 times weaker than that of the original desolvated form of **Eu-FJU6**. Significantly, in the case of **Eu-FJU6**⊃Co^{2+}, the $^5D_0 \rightarrow {}^7F_2$ luminescence intensity (615 nm) for a 0.5 mol L^{-1} solution was about 17 times weaker than that of the original desolvated form of **Eu-FJU6**.

The results of the cation-dependent luminescence quenching effect indicated that the desolvated form of **Eu-FJU6** could serve as a potential candidate for modulating the luminescence

Fig. 7. (up)

Fig. 7. (bottom)

Fig. 7. Comparison of the PL intensity at 615 nm ($^5D_0 \rightarrow {}^7F_2$ transition) for cation-inclusion samples of the **Eu-FJU6**⊃cation prepared using two different concentrations of cation solutions. The cation-inclusion samples of **Eu-FJU6**⊃cation was prepared by introducing 80 mg of desolvated **Eu-FJU6** (refluxing with water at 90 °C for 24 hours.) into 30 ml of metal ion aqueous solution with different amounts of $M(NO_3)_x$ (x = 1 or 2, M = Na^+, Co^{2+}, Ni^{2+}, Cu^{2+}, Zn^{2+}, Cd^{2+}), and collected by filtration with deionized water and dried under aerobic conditions for 3 days. (λ_{ex} = 368 nm, up: 0.5 mol L^{-1}; bottom: 0.25 mol L^{-1}; **Std**.: represents the desolvated **Eu-FJU6**.)

behaviour experienced by small amounts of Ni^{2+} or Co^{2+} ions in aqueous solutions. The highly selective luminescent sensors induced by modulation are of great interest owing to their potential for use in recognizing a diversity of guest molecules through specific host-guest interactions.[25–26]

The *Stern-Volmer* equation was applied quantitatively, in an attempt to develop a better understanding of the quenching effect of Ni^{2+} and Co^{2+} ions:

$$\frac{I_0}{I} = 1 + K_{SV}[M]$$

the value of I_0 is the luminescence intensity of desolvated **Eu-FJU6**, and the value of I is the luminescence intensity of **Eu-FJU6**⊃Ni^{2+} and **Eu-FJU6**⊃Co^{2+}. [*M*] is the molar concentration of the cation. K_{sv} is the quenching effect coefficient of the cation.

Fig. 8a.

Fig. 8b.

Fig. 8. PL spectra of **Eu-FJU6**⊃cation in the presence of various concentrations of: (a) Ni^{2+}; (b) Co^{2+} ions when excited at 368 nm. (**Std**. represents desolvated **Eu-FJU6**)

The K_{sv} value for Ni^{2+} ions was determined to be 8.7 M^{-1}, which was about 4 times weaker than that of Co^{2+} ions with a K_{sv} value of 33.0 M^{-1}, indicating that the ability of recognition of Co^{2+} ions through the Lewis basic carboxylate oxygen sites within the 3D framework is better than that for Ni^{2+} ions through the possible quenching mechanism proposed by Chen *at el*.[12b]

It is interesting to note that the K_{sv} value for dilute solutions of **Eu-FJU6**⊃Ni^{2+} deviated from the linear *Stern-Volmer* equation, indicating that the cation-dependent luminescence quenching effect was less efficient than that for **Eu-FJU6**⊃Co^{2+}. That the luminescence intensity of **Eu-FJU6**⊃Ni^{2+} was not proportional to the concentration of Ni^{2+} suggests that the quenching effect would become negligible, when overrich Ni^{2+} ions began to perturb the coordination spheres of the Eu^{3+} ions within the 3D framework, as evidenced by a strong ligand centered emission at 425–550 nm in Fig. S12a.†

In contrast to **Eu-FJU6**⊃Ni^{2+}, the luminescence modulation data for dilute solutions of **Eu-FJU6**⊃Co^{2+} were in good agreement with the *Stern-Volmer* equation, and moreover, as shown in Fig. S12b,† the ligand centered emission at 425–550 nm of **Eu-FJU6**⊃Co^{2+} was much weaker than that of **Eu-FJU6**⊃Ni^{2+}, clearly demonstrating the existence of interactions between Co^{2+} ions and the Lewis basic carboxylate sites for the desolvated **Eu-**

FJU6, as detected *via* the luminescence modulation approach. In the case of less perturbation of the coordination spheres of Eu^{3+} ions after the modulation experiments, the Co^{2+}-dependent luminescence quenching effect of the desolvated form of **Eu-FJU6** was comparable with that for cation signaling effects reported in the literature.[25]

Although the degree of sensitivity to Ni^{2+} and Co^{2+} ions was relatively moderate, it should be noted that: (1) the active Eu^{3+} centers embedded in the 3D frameworks lend themselves to luminescence modulation, which was accomplished by the Lewis carboxylate sites on the pore channels; (2) the active Eu^{3+} centers were further stabilized by the carboxylate shift, which prevented active Eu^{3+} centers from being coordinated by water molecules in aqueous solution, suggesting that vibrational quenching induced by O—H oscillations in water molecules is prohibited.[24,27] As a consequence, Ni^{2+} / Co^{2+} ions-induced luminescence modulation provides **Eu-FJU6** an appropriate approach for potentially applying its porosity to further sensing functions. Different from previously explored LnOFs featuring anionic, fluorinated, —OH group-decorated frameworks,[25b,27–28] the 3D frameworks of **Eu-FJU6**, however, are characterized solely by the organic ligand of 2,6-NDC, which permit the Lewis basic carboxylate sites to modulate the luminescence of Ni^{2+} / Co^{2+} ions in aqueous solution.

Conclusions

Four novel 3D pillar-supported packed double-decker lanthanide-based metal—organic frameworks **Ln-FJU6** (**Ln** = Ce, Pr, Nd, and Eu) were successfully synthesized by the reaction of 2,6-naphthalenedicarboxylic acid and lanthanide nitrates under mild hydrothermal conditions. **Ln-FJU6** exhibits unusual arrays of 2D intersecting channels between the adjacent packed double-decker architectures within the host frameworks. The high coordination number of lanthanides, the strong metal-carboxylate bonding, and the π—π interactions between the closely stacked naphthalene rings of the NDC^{I} ligands contribute to the high thermal stability of the host frameworks of **Ln-FJU6**. Significantly, cation-induced luminescence modulation is observed for the desolvated form of **Eu-FJU6**, which serves as a potential candidate for experiencing small amounts Co^{2+} ions in aqueous solution through luminescence modulation as a result of metal–Lewis basic carboxylate site interactions. Further studies in this category are currently under way.

Acknowledgement

The financial support for this work from Fu Jen Catholic University and National Science Council of Taiwan are gratefully acknowledged.

Notes and references

Department of Chemistry, Fu Jen Catholic University, New Taipei City 24205, Taiwan. Fax: +886-2-29023209; E-mail: 056461@mail.fju.edu.tw

† Electronic Supplementary Information (ESI) available: [details of any supplementary information available should be included here]. See DOI: 10.1039/b000000x/

1 (a) M. D. Allendorf, C. A. Bauer, R. K. Bhakta and R. J. T. Houk, *Chem. Soc. Rev.*, 2009, **38**, 1330; (b) M. Kurmoo, *Chem. Soc. Rev.*, 2009, **38**, 1353; (c) C.-Y. Sun, X.-L. Wang, X. Zhang, C. Qin, P. Li, Z.-M. Su, D.-X. Zhu, G.-G. Shan, K.-Z. Shao, H. Wu, J. Li, *Nat. Commun.*, 2013, **4**:2717.

2 (a) J. D. Rocca, D. Liu and W. Lin, *Acc. Chem. Res.*, 2011, **44**, 957; (b) S. V. Eliseeva and J.-C. G. Bünzli, *Chem. Soc. Rev.*, 2010, **39**, 189; (c) N. Stock and S. Biswas, *Chem. Rev.*, 2012, **112**, 933; (d) W. J. Rieter, K. M. L. Taylor and W. Lin, *J. Am. Chem. Soc.*, 2007, **129**, 9852; (e) K. M. L. Taylor, A. Jin and W. Lin, *Angew. Chem. Int. Ed.*, 2008, **47**, 7722; (f) J. D. Rocca and W. Lin, *Eur. J. Inorg. Chem.*, 2010, 3725; (g) C. Wang, D. Liu and W. Lin, *J. Am. Chem. Soc.*, 2013, **135**, 13222; (h) K. M. L. Taylor-Pashow, J. D. Rocca, Z. Xie, S. Tran and W. Lin, *J. Am. Chem. Soc.*, 2009, **131**, 14261.

3 (a) L. D. Carlos, R. A. S. Ferreira, V. D. Z. Bermudez, and S. J. L. Ribeiro, *Adv. Mater.*, 2009, **21**, 509; (b) C. Serre, F. Millange, C. Thouvenot, N. Gardant, F. Pellé and G. Férey, *J. Matter. Chem.*, 2004, **14**, 1540; (c) P. Falcaro and S. Furukawa, *Angew. Chem. Int. Ed.*, 2012, **51**, 8431 ; (d) N. Kerbellec, D. Kustaryono, V. Haquin, M. Etienne, C. Daiguebonne and O. Guillou, *Inorg. Chem.*, 2009, **48,** 2837; (e) D. T. D. Lill, A. D. Bettencourt-Dias and C. L. Cahill, *Inorg. Chem.*, 2007, **46**, 3960; (f) Y. Zeng, Z. Li, Y. Liang, X. Gan and M. Zheng, *Inorg. Chem.*, 2013, **52**, 9590; (g) M.-S. Wang, S.-P. Guo, Y. Li, L.-Z. Cai, J.-P. Zou, G. Xu, W.-W. Zhou, F.-K. Zheng and G.-C. Guo, *J. Am. Chem. Soc.*, 2009, **131**, 13572; (h) D. F. Sava, L. E. S. Rohwer, M. A. Rodriguez and T. M. Nenoff, *J. Am. Chem. Soc.*, 2012, **134**, 3983; (i) X. Rao, Q. Huang, X. Yang, Y. Cui, Y. Yang, C. Wu, B. Chen and G. Qian, *J. Mater. Chem.*, 2012, **22**, 3210; (j) S. Dang, J.-H. Zhang and Z.-M. Sun, *J. Mater. Chem.*, 2012, **22**, 8868.

4 (a) L. E. Kreno, K. Leong, O. K. Farha, M. Allendorf, R. P. V. Duyne and J. T. Hupp, *Chem. Rev.*, 2012, **112**, 1105; (b) Y. Cui, Y. Yue, G. Qian and B. Chen, *Chem. Rev.*, 2012, **112**, 1126; (c) J. Rocha, L. D. Carlos, F. A. A. Paz and D. Ananias, *Chem. Soc. Rev.*, 2011, **40**, 926; (d) O. Shekhah, J. Liu, R. A. Fischer and C. Wöll, *Chem. Soc. Rev.*, 2011, **40**, 1081; (e) D. Zacher, O. Shekhah, C. Wöll and R. A. Fischer, *Chem. Soc. Rev.*, 2009, **38**, 1418; (f) M. Meilikhov, S. Furukawa, K. Hirai, R. A. Fischer and S. Kitagawa, *Angew. Chem. Int. Ed.*, 2013, **52**, 341; (g) D. Buso, J. Jasieniak, M. D. H. Lay, P. Schiavuta, P. Scopece, J. Laird, H. Amenitsch, A. J. Hill and P. Falcaro, *small*, 2012, **8**, 80; (h) H. Hosseini, H. Ahmar, A. Dehghani, A. Bagheri, A. Tadjarodi and A. R. Fakhari, *Biosens. Bioelectron.*, 2013, **42**, 426; (i) T. Lee, H. L. Lee, M. H. Tsai, S.-L. Cheng, S.-W. Lee, J.-C. Hu and L.-T. Chen, *Biosens. Bioelectron.*, 2013, **43**, 56; (j) X. J. Zhao, R. X. He and Y. F. Li, *Analyst*, 2012, **137**, 5190; (k) M. Zheng, H. Tan, Z. Xie, L. Zhang, X. Jing and Z. Sun, *ACS Appl. Mater. Interfaces*, 2013, **5**, 1078.

5 W.-G. Lu, L. Jiang and T.-B. Lu, *Cryst. Growth Des.*, 2010, **10**, 4310.

6 G. Férey, *Chem. Mater.*, 2001, **13**, 3084.

7 (a) P. Mahata, K. V. Ramya and S. Natarajan, *Chem. Eur. J.*, 2008, **14**, 5839; (b) A. Michaelides, S. Skoulika, E. G. Bakalbassis and J. Mrozinski, *Cryst. Growth Des.*, 2003, **3**, 487; (c) P. Zhu, W. Gu, M.-L. Liu, H.-B. Song, X. Liu, Y.-Q. Gao, H.-Y. Duan, S.-P. Yan and D.-Z. Liao, *CrystEngComm*, 2009, **11**, 351; (d) J. Liang, R. Ma, Y. Ebina, F. Geng and T. Sasaki, *Inorg. Chem.*, 2013, **52**, 1755; (e) P. Silva, L. Cunha-Silva, N. J. O. Silva, J. Rocha and F. A. A. Paz, *Cryst. Growth Des.*, 2013, **13**, 2607; (f) Z. Min, M. A. Singh-Wilmot, C L. Cahill, M Andrews and R Taylor, *Eur. J. Inorg. Chem.*, 2012, **2012**, 4419; (g) Y. Gao, Y. Xu, Z. Han, C. Li, F. Cui, Y. Chi and C. Hu, *J. Solid State Chem.*, 2010, **183**, 1000; (h) G. Huang, P. Yang, N. Wang, J.-Z. Wu and Y. Yu, *Inorg. Chim. Acta*, 2012, **384**, 333; (i) Q. Sun, J.-Y. Zhang, H. Tian, Y.-Q. Wang and E.-Q. Gao, *Inorg. Chem. Commun.*, 2009, **12**, 426; (j) L. Cheng, S. Gou and G. Xu, *J. Mol. Struct.*, 2010, **979**, 214; (k) S. Mohapatra, S. Vayasmudri, G. Mostafa, T. K. Maji, *J. Mol. Struct.*, 2009, **932**, 123; (l) J. Xu, W. Su and M. Hong, *Inorg. Chem. Commun.*, 2011, **14**, 1794.

8 (a) W.-G. Lu, D.-C. Zhong, L. Jiang and T.-B. Lu, *Cryst. Growth Des.*, 2012, **12**, 3675; (b) Z. Chen, B. Zhao, Y. Zhang, W. Shi and P. Cheng, *Cryst. Growth Des.*, 2008, **8**, 2291; (c) Z.-P. Deng, L.-H. Huo, H.-Y. Wang, S. Gao and H. Zhao, *CrystEngComm*, 2010, **12**, 1526; (d) Y.-Q. Sun, Q. Liu, J.-C. Zhong, Q.-F. Pan and Y.-P. Chen, *J. Solid State Chem.*, 2013, **206**, 85; (e) Z.-G. Gu, M.-F Wang, H.-M.

Peng, G.-Z. Li, X.-Y. Yi, X. Gong, H.-C. Fang, Z.-Y. Zhou and Y.-P. Cai, *Inorg. Chem. Commun*., 2010, **13**, 1439.
9 (a) J. Xia, B. Zhao, H.-S. Wang, W. Shi, Y. Ma, H.-B. Song, P. Cheng, D.-Z. Liao and S.-P. Yan, *Inorg. Chem*., 2007, **46**, 3450; (b) X. Feng, J. Wang, B. Liu, L. Wang, J. Zhao and S. Ng, *Cryst. Growth Des*., 2012, **12**, 927.
10 (a) V. A. Russell, C. C. Evans, W. Li and M. D. Ward, *Science*, 1997, **276**, 575; (b) S. Kitagawa, R. Kitaura and S.-I. Noro, *Angew. Chem. Int. Ed*., 2004, **43**, 2334; (c) K. T. Holman, A. M. Pivovar, J. A. Swift and M. D. Ward, *Acc. Chem. Res*., 2001, **34**, 107; (d) H. J. Choi and M. P. Suh, *J. Am. Chem. Soc*., 2004, **126**, 15844.
11 (a) X.-Y. Chen, B. Zhao, W. Shi, J. Xia, P. Cheng, D.-Z. Liao, S.-P. Yan and Z.-H. Jiang, *Chem. Mater*., 2005, **17**, 2866; (b) C.-H. Li, K.-L. Huang, Y.-N. Chi, X. Liu, Z.-G. Han, L. Shen and C.-W. Hu, *Inorg. Chem*., 2009, **48**, 2010; (c) S.-P. Chen, Y.-X. Ren, W.-T. Wang and S.-L. Gao, *Dalton Trans*., 2010, **39**, 1552; (d) L. Zhang, N. Yu, K. Zhang, R. Qiu, Y. Zhao, W. Rong and H. Deng, *Inorg. Chem. Acta*, 2013, **400**, 67.
12 (a) B. Chen, L. Wang, Y. Xiao, F. R. Fronczek, M. Xue, Y. Cui and G. Qian, *Angew. Chem. Int. Ed*., 2009, **48**, 500; (b) Y. Xiao, Y. Cui, Q. Zheng, S. Xiang, G. Qian and B. Chen, *Chem. Commun*., 2010, **46**, 5503;
13 *SAINT*, Bruker (2003). Bruker AXS Inc., Madison, Wisconsin, USA.
14 *SADABS*, Bruker (2002). Bruker AXS Inc., Madison, Wisconsin, USA.
15 G. M. Sheldrick, *Acta Crystallogr*., *Sect. A*: *Found. Crystallogr*., 2008, **64**, 112.
16 (a) J.-P. Zhang, X.-C. Huang and X.-M. Chen, *Chem. Soc. Rev*., 2009, **38**, 2385; (b) N. W. Ockwig, O. Delgado-Fsiedrichs, M. O'Keeffe and O. M. Yaghi, *Acc. Chem. Res*., 2005, **38**, 176; (c) J.-Y. Wu, S.-L. Yang, T.-T. Luo, Y.-H. Liu, Y.-W. Cheng, Y.-F. Chen, Y.-S. Wen, L.-G. Lin and K.-L. Lu, *Chem. Eur. J*., 2008, **14**, 7136; (d) C.-P. Li, Q. Yu, J. Chen and M. Du, *Cryst. Growth Des*., 2010, **10**, 2650; (e) H.-L. Jiang, Y. Tatsu, Z.-H. Lu and Q. Xu, *J. Am. Chem. Soc.*, 2010, **132**, 5586; (f) A. K. Cheetham, C. N. R. Rao and R. K. Feller, *Chem. Commun*., 2006, **46**, 4780; (g) A.-X. Tian, J. Ying, J. Peng, J.-Q. Sha, H.-J. Pang, P.-P. Zhang, Y. Chen, M. Zhu and Z.-M. Su, *Inorg. Chem.*, 2009, **48**, 100.
17 (a) Z. Wang, C.-M. Jin, T. Shao, Y.-Z. Li, K.-L. Zhang, H.-T. Zhang and X.-Z. You, *Inorg. Chem. Commun*., 2002, **5**, 642; (b) X. Zheng, C. Sun, S. Lu, F. Liao, S. Gao and L. Jin, *Eur. J. Inorg. Chem*., 2004, **2004**, 3262; (c) X.-J. Zheng, Z.-M. Wang, S. Gao, F.-H. Liao, C.-H. Yan and L.-P. Jin, *Eur. J. Inorg. Chem*., 2004, **2004**, 2968.
18 A. L. Spek, *PLATON*, *A Multipurpose Crystallographic Tool*, Utrecht University, Utrecht, The Netherlands, 2005.
19 (a) D.-C. Hou, G.-Y. Jiang, Z. Zhao and J. Zhang, *Inorg. Chem. Commun*., 2013, **29**, 148; (b) L.-S. Long, R.-B. Huang, Q.-Q. Kang and L.-S. Zheng, *Private Communication*, 2006
20 (a) J.-Y. Wu, T.-T. Yeh, Y.-S. Wen, J. Twu and K.-L. Lu, *Cryst. Growth Des*., 2006, **6**, 467; (b) Y.-H. Liu, Y.-L. Lu, H.-C. Wu, J.-C. Wang and K.-L. Lu, *Inorg. Chem.*, 2002, **41**, 2592; (c) S. S.-Y. Chui, S. M.-F. Lo, J. P. H. Charmant, A. G. Orpen and I. D. Williams, *Science*, 1999, **283**, 1148.
21 (a) C. A. Hunter and J. K. M. Sanders, *J. Am. Chem. Soc*., 1990, **112**, 5525; (b) H. R. Khavasi and M. A. Fard, *Cryst. Growth Des*., 2010, **10**, 1892.
22 (a) R. Łyszczek, Z. Rzączyńska, A. Kula, A. Gładysz-Płaska, *J. Anal. Appl. Pyrolysis*, 2011, **92**, 347; (b) Q.-Y. Liu, W.-F. Wang, Y.-L. Wang, Z.-M. Shan, M.-S. Wang and J. Tang, *Inorg. Chem*., 2012, **51**, 2381; (c) N. Li, L. Gou, H.-M. Hu, S.-H. Chen, X.-L. Chen, B.-C. Wang, Q.-R. Wu, M.-L. Yang and G.-L. Xue, *Inorg. Chem. Acta*, 2009, **362**, 3475.
23 (a) *Lanthanide and Actinide Chemistry*, ed. S. Cotton, John Wiley & Sons, England, 2006; (b) *Lanthanide Probes in Life*, *Chemical and Earth Sciences*: *Theory and Practice*, ed. J.-C. G. Bünzli and G. R. Choppin, Elsevier, Netherlands, 1989; (c) K. Binnemans and C. Gorllerwalrand, *J. Rare Earths*, 1996, **14**, 173; (d) J. C. G. Bunzli and C. Piguet, *Chem. Soc. Rev*., 2005, **34**, 1048; (e) M. O. Rodrigues, N. B. da Costa, C. A. de Simone, A. A. S. Araújo, A. M. Brito-Silva, F. A. A. Paz, M. E. de Mesquita, S. A. Júnior and R. O. Freire, *J. Phys. Chem. B*, 2008, **112**, 4204; (f) K. Binnemans, *Chem. Rev*., 2009, **109**, 4283.
24 A. M. Kłonkowski, S. Lis, M. Pietraszkiewicz, Z Hnatejko, K. Czarnobaj and M. Elbanowski, *Chem. Mater*., 2003, **15**, 656.
25 (a) W. Liu, T. Jiao, Y. Li, Q. Liu, M. Tan, H. Wang and L. Wang, *J. Am. Chem. Soc*., 2004, **126**, 2280; (b) W.-G. Lu, L. Jiang, X.-L. Feng and T.-B. Lu, *Inorg. Chem*., 2009, **48**, 6997; (c) X.-Q. Zhao, B. Zhao, W. Shi and P. Cheng, *CrystEngComm*, 2009, **11**, 1261; (d) B. Zhao, X.-Y. Chen, Z. Chen, W. Shi, P. Cheng, S.-P. Yan and D.-Z. Liao, *Chem. Commun*., 2009, 3113; (e) B. Zhao, H.-L. Gao, X.-Y. Chen, P. Cheng, W. Shi, D.-Z. Liao, S.-P. Yan and Z.-H. Jiang, *Chem. Eur. J*., 2006, **12**, 149; (f) Y.-M. Zhu, C.-H. Zeng, T.-S. Chu, H.-M. Wang, Y.-Y. Yang, Y.-X Tong, C.-Y. Su and W.-T. Wong, *J. Mater. Chem. A*, 2013, **1**, 11312; (g) S. Dang, E. Ma, Z.-M. Sun and H. Zhang, *J. Mater. Chem*., 2012, **22**, 16920; (h) Q. Tang, S. Liu, Y. Liu, J. Miao, S. Li, L. Zhang, Z. Shi and Z. Zheng, *Inorg. Chem*., 2013, **52**, 2799.
26 (a) B. Chen, S. Xiang and G. Qian, *Acc. Chem. Res.*, 2010, **43**, 1115; (b) A. Lan, K. Li, H. Wu, D. H. Olson, T. J. Emge, W. Ki, M. Hong and J. Li, *Angew. Chem. Int. Ed*., 2009, **48**, 2334; (c) Y. Li, S. Zhang and D. Song, *Angew. Chem. Int. Ed*., 2013, **52**, 710; (d) Y. K. Park, S. B. Choi, H. Kim, K. Kim, B.-H. Won, K. Choi, J.-S. Choi, W.-S. Ahn, N. Won, S. Kim, D. H. Jung, S.-H. Choi, G.-H. Kim, S.-S. Cha, Y. H. Jhon, J. K. Yang and J. Kim, *Angew. Chem. Int. Ed*., 2007, **46**, 8230; (e) Z. Guo, H. Xu, S. Su, J. Cai, S. Dang, S. Xiang, G. Qian, H. Zhang, M. O'Keeffe and B. Chen, *Chem. Commun*., 2011, **47**, 5551.
27 K.-L. Wong, G.-L. Law, Y.-Y. Yang and W.-T. Wong, *Adv. Mater*., 2006, **18**, 1051.
28 B. Chen, Y. Yang, F. Zapata, G. Qian, Y. Luo, J. Zhang and E. B. Lobkovsky, *Inorg. Chem*., 2006, **45**, 8882.

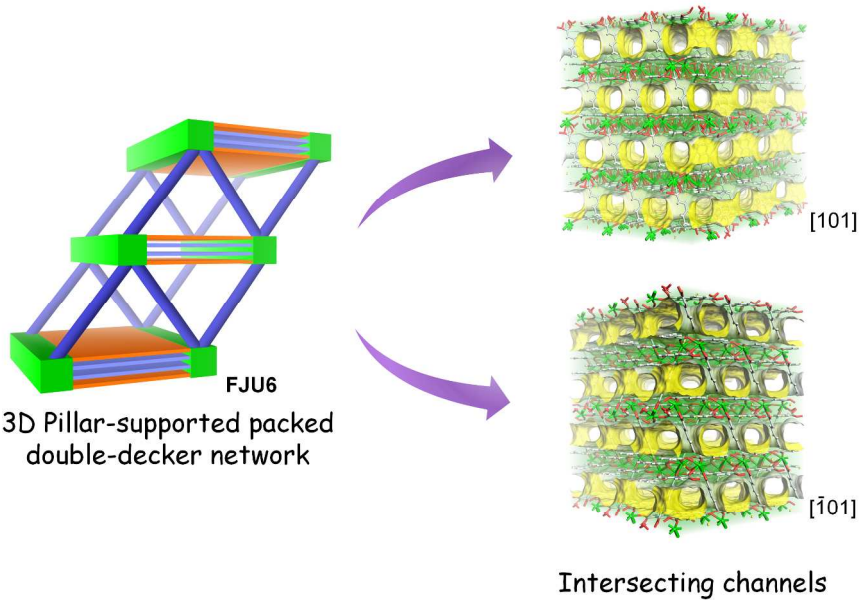

800x500mm (96 x 96 DPI)

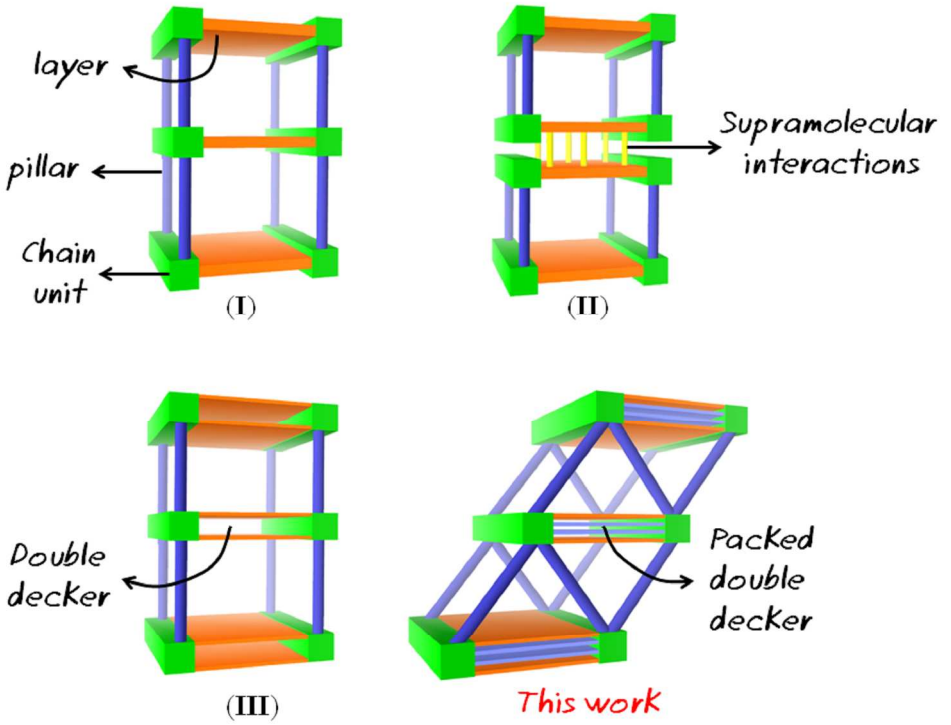

523x392mm (96 x 96 DPI)

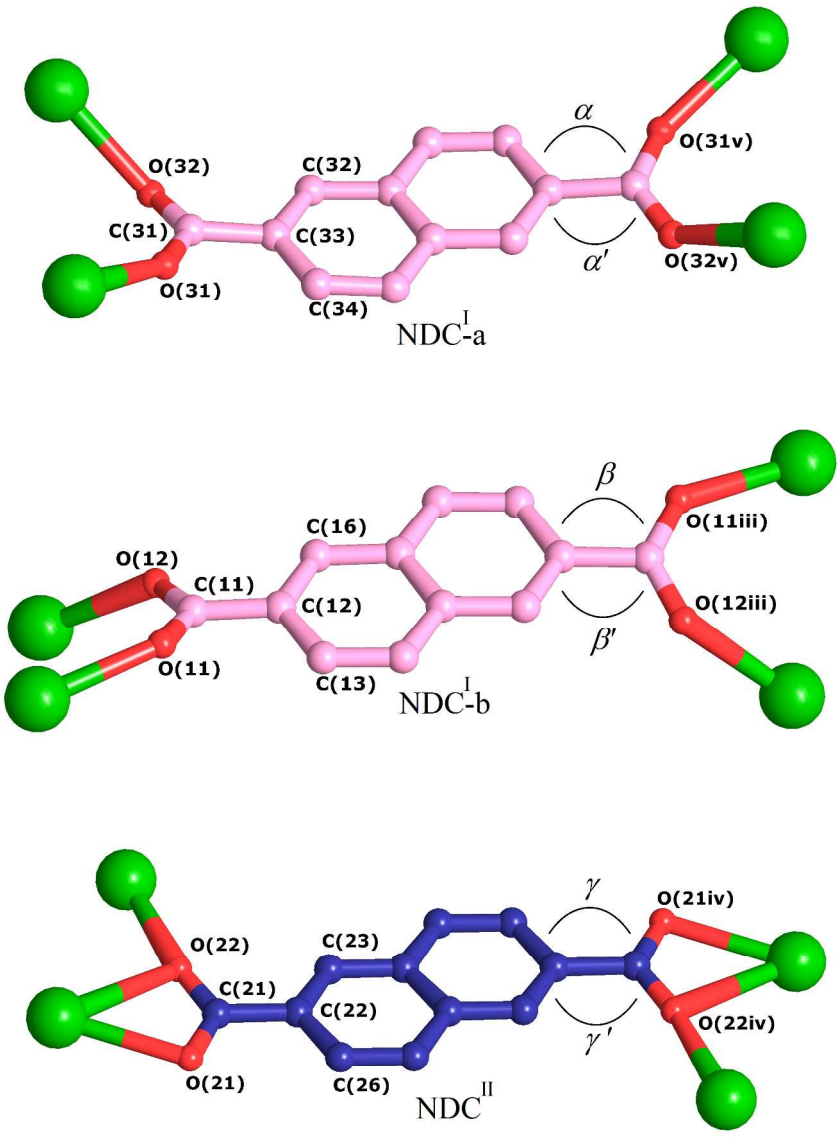

770x977mm (96 x 96 DPI)

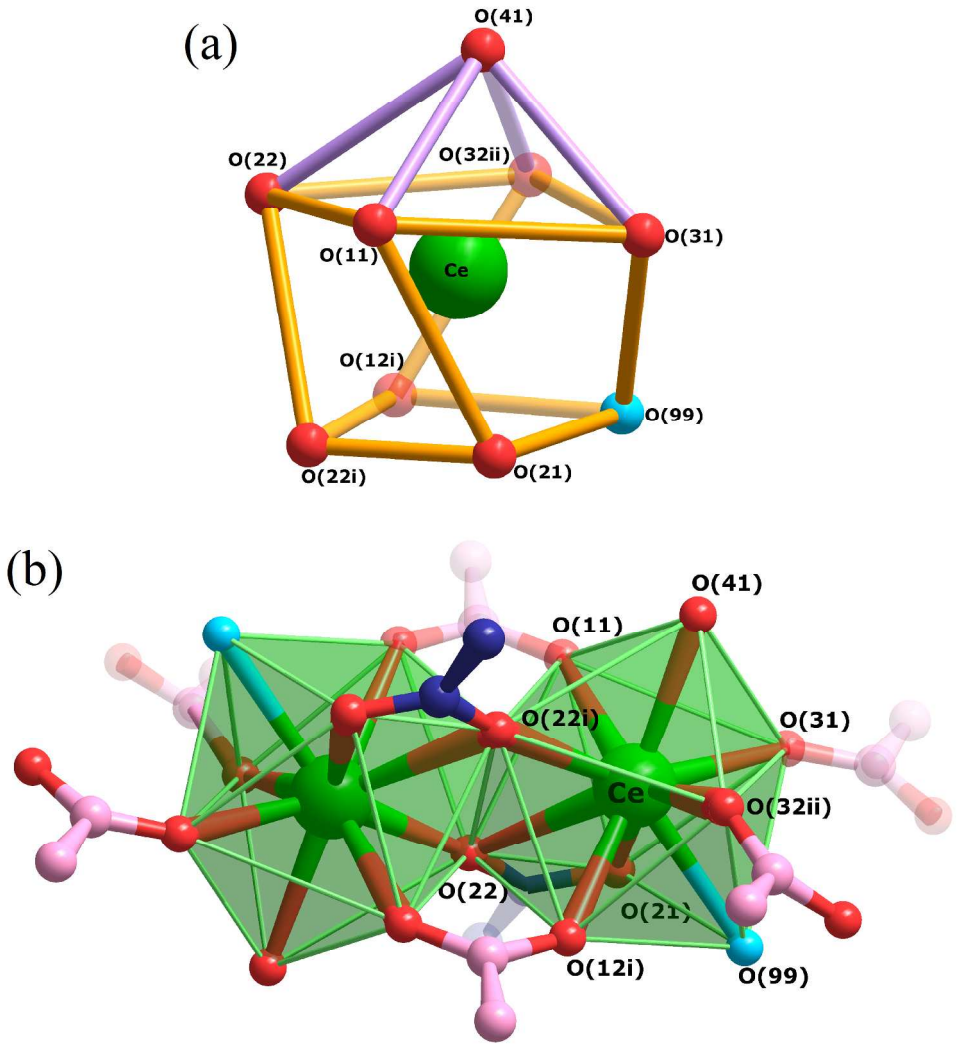

990x1047mm (96 x 96 DPI)

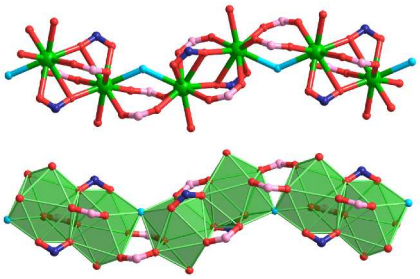

1D Ce–carboxylate cluster chains

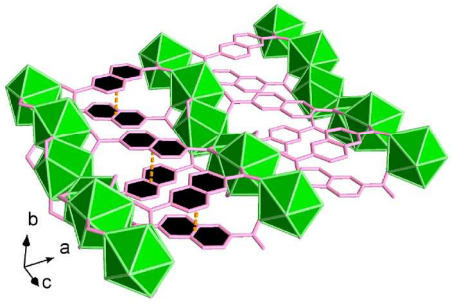

2D Packed double decker

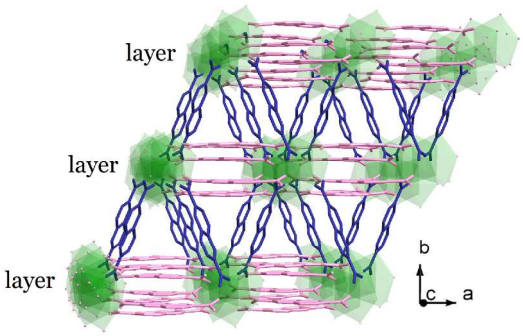

3D Pillar-supported double decker

876x1911mm (96 x 96 DPI)

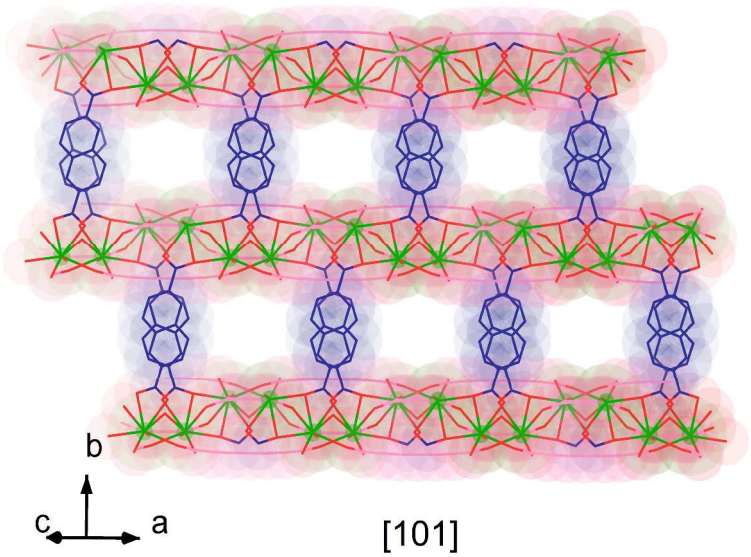

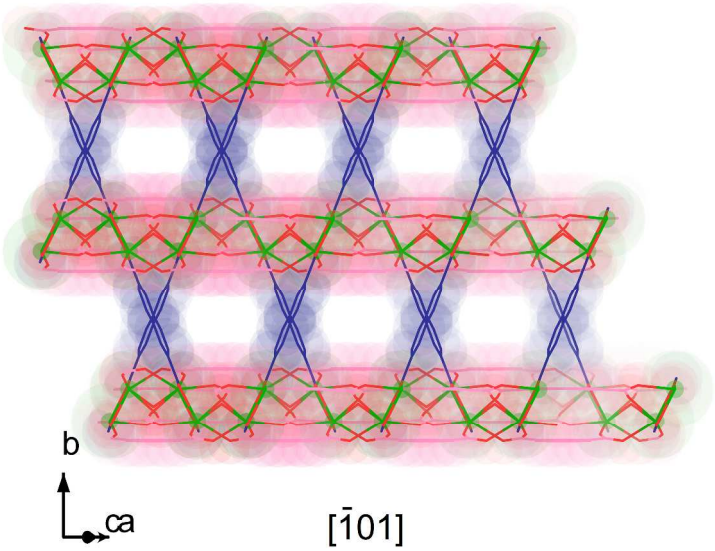

1079x1638mm (96 x 96 DPI)

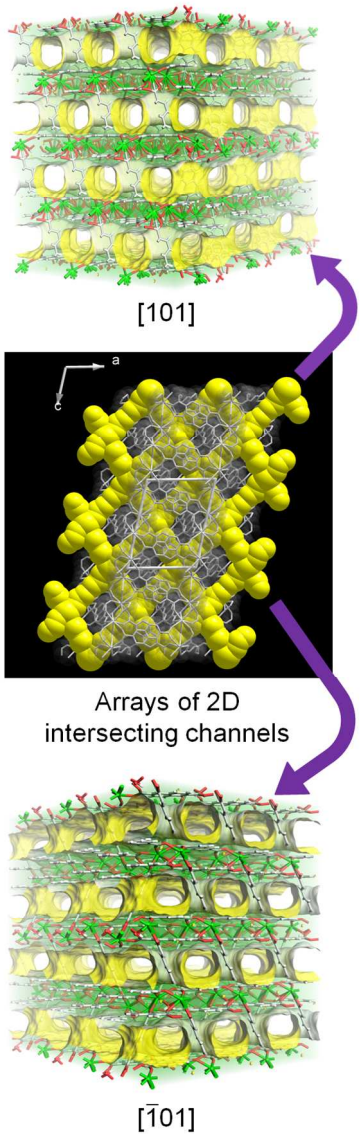

200x550mm (96 x 96 DPI)

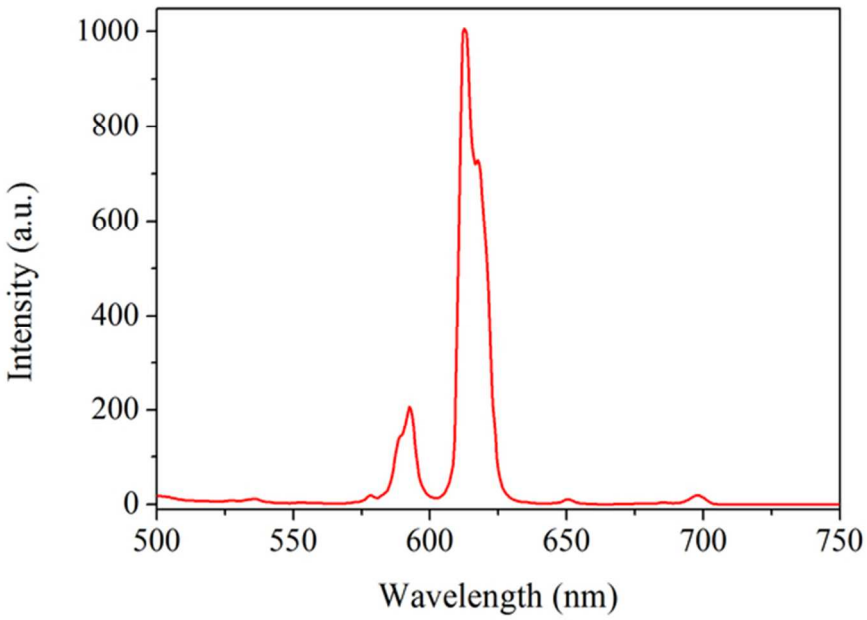

59x41mm (300 x 300 DPI)

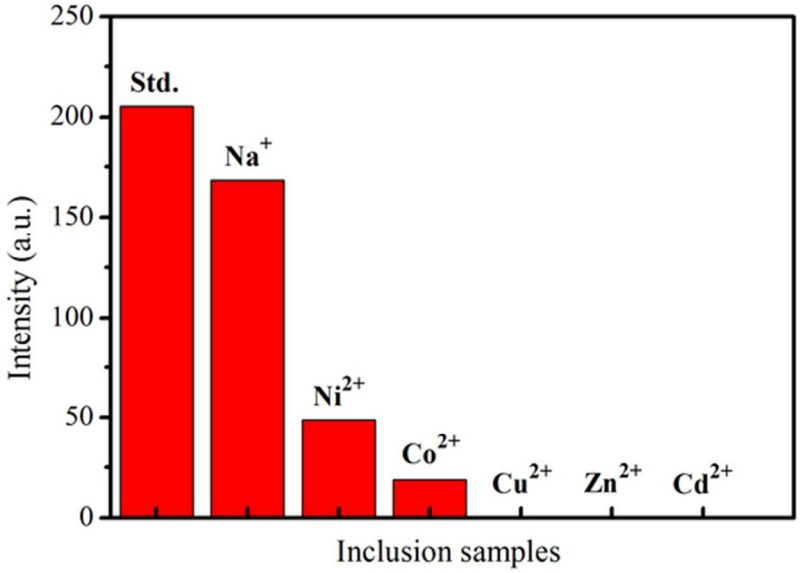

59x41mm (300 x 300 DPI)

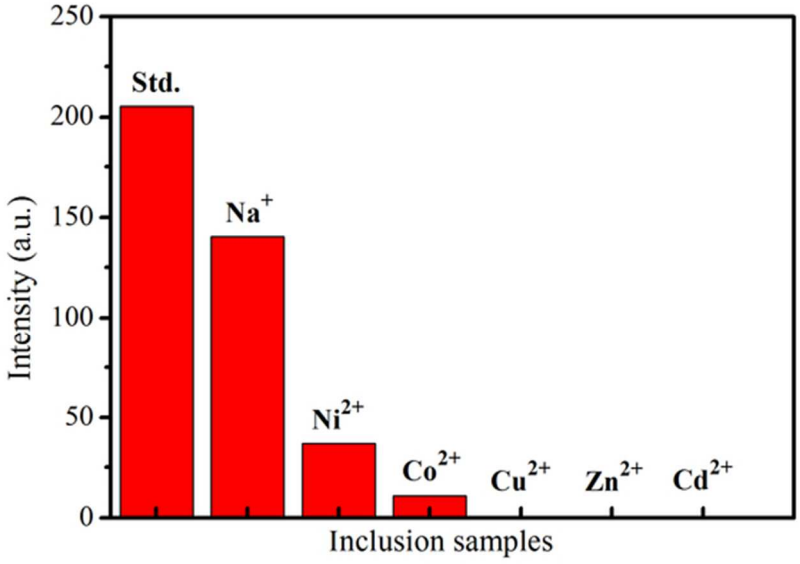

59x41mm (300 x 300 DPI)

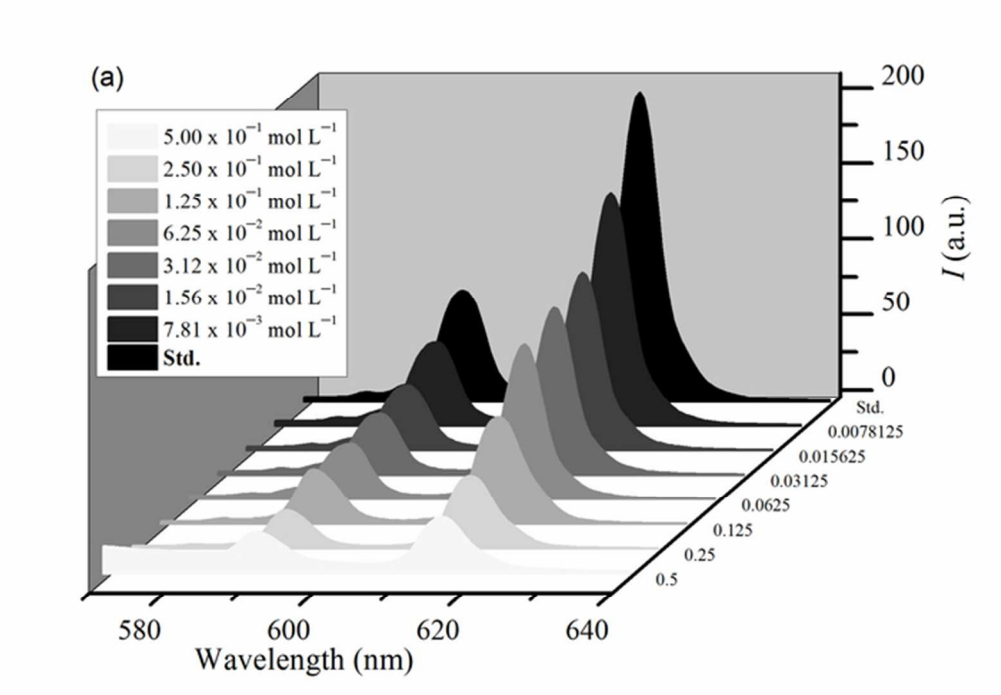

59x41mm (300 x 300 DPI)

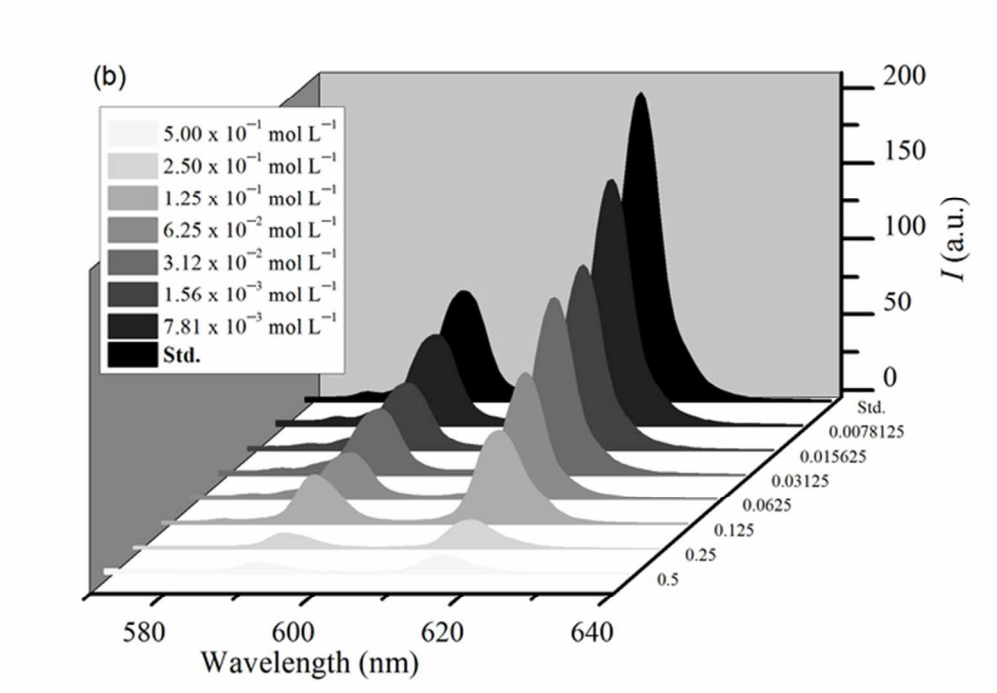

59x41mm (300 x 300 DPI)